energies

MDPI

Article

Application of Battery Energy Storage Systems for Primary Frequency Control in Power Systems with High Renewable Energy Penetration

Md Ruhul Amin *, Michael Negnevitsky, Evan Franklin, Kazi Saiful Alam and Seyed Behzad Naderi

Centre for Renewable Energy and Power Systems, School of Engineering, University of Tasmania (UTAS), Hobart, TAS 7005, Australia; Michael.Negnevitsky@utas.edu.au (M.N.); evan.franklin@utas.edu.au (E.F.); kazi.alam@utas.edu.au (K.S.A.); Seyedbehzad.Naderi@utas.edu.au (S.B.N.)

* Correspondence: mdruhul.amin@utas.edu.au

Abstract: In power systems, high renewable energy penetration generally results in conventional synchronous generators being displaced. Hence, the power system inertia reduces, thus causing a larger frequency deviation when an imbalance between load and generation occurs, and thus potential system instability. The problem associated with this increase in the system's dynamic response can be addressed by various means, for example, flywheels, supercapacitors, and battery energy storage systems (BESSs). This paper investigates the application of BESSs for primary frequency control in power systems with very high penetration of renewable energy, and consequently, low levels of synchronous generation. By re-creating a major Australian power system separation event and then subsequently simulating the event under low inertia conditions but with BESSs providing frequency support, it has been demonstrated that a droop-controlled BESS can greatly improve frequency response, producing both faster reaction and smaller frequency deviation. Furthermore, it is shown via detailed investigation how factors such as available battery capacity and droop coefficient impact the system frequency response characteristics, providing guidance on how best to mitigate the impact of future synchronous generator retirements. It is intended that this analysis could be beneficial in determining the optimal BESS capacity and droop value to manage the potential frequency stability risks for a future power system with high renewable energy penetrations.

Keywords: battery storage; primary frequency control; synchronous generator retirement; high renewable energy penetration; non-synchronous generating sources; National Electricity Market; Australian energy market operator; integrated system plan

Citation: Amin, M.R.; Negnevitsky, M.; Franklin, E.; Alam, K.S.; Naderi, S.B. Application of Battery Energy Storage Systems for Primary Frequency Control in Power Systems with High Renewable Energy Penetration. *Energies* **2021**, *14*, 1379. https://doi.org/10.3390/en14051379

Academic Editor: Teuvo Suntio

Received: 29 January 2021
Accepted: 26 February 2021
Published: 3 March 2021

1. Introduction

The deployment of power generation sourced from Renewable Energy (RE) is growing steadily, as power systems around the world transition to being based around low-carbon technologies. This deployment generally occurs via the replacement of conventional Synchronous Generators (SGs), which creates many great challenges in power systems [1]. In Australia, for example, the Integrated System Plan (ISP) published by the Australian Energy Market Operator (AEMO) provides a roadmap for eastern Australia's power system to optimise consumer benefits through a transition period of great complexity and uncertainty [2,3]. ISP findings highlighted the anticipated transformation of the generation mix in the National Electricity Market (NEM) of Australia by 2040. A substantial closure of coal-fired generation fleets is expected, with the future NEM generation mix driven by factors such as the withdrawal of ageing generation assets, reduced carbon emission policies, and changing demand patterns [2,3].

The NEM will draw on a technological mix that may diversify even further as other technologies mature and become commercially competitive to the current generation. Specifically, approximately 60% of the coal-fired generation fleet is expected to be exiting

the NEM generation mix by 2040, and RE non-synchronous generating sources (NSGSs) such as wind and solar are likely to make up their replacements [3]. Therefore, Australia's power system, and many others like it, will experience a considerable reduction in system inertia, which can lead to increased power system frequency deviations and potentially even instability and blackouts [4].

The increasing frequency deviation can be mitigated by several means, including battery energy storage systems (BESSs), which have already demonstrated their capability to provide primary frequency support for low inertia power systems [5–8]. Lee et al. [9] demonstrated that distributed BESS, controlled by coordinated control algorithms, can minimise frequency deviations by up to 50% following a critical event in the Korean power system. A distributed control strategy for coordinating multiple BESSs to support frequency regulation in power systems with high penetration of renewable generation is proposed by Zhao et al. [10]. A droop-type, lead-lag controlled BESSs is proposed by Datta et al. [6] to provide additional damping of the system with around 18% PV penetration while satisfying the NEM regulatory requirements. Amin et al. [11] presented a comparison of power system frequency response is presented for a simplified power system with primary frequency control (PFC) being provided by either synchronous generators or BESS. Amin et al. [11] demonstrated that BESS enabled for PFC is capable of eliminating frequency undershoot and reducing settling time by 70%, after a major contingency event in a power system containing various types of conventional generation technologies. In this work, we provide a systematic analysis of the performance of droop-controlled BESS in power systems with high and very high RE NSGS penetration, by assessing system frequency response as a function of BESS capacity and droop characteristics.

Until now, BESS dynamic response research has mostly focused on demonstrating the role of BESS in improving generally the frequency stability under high RE NSGS penetration [6,12,13]. However, as yet, little emphasis has been placed on providing a systematic assessment of the BESS characteristics required to meet a desired frequency standard. Transient stability enhancement capability of BESSs for a large-scale power system is investigated by Datta et al. [14]. The capability of BESS to reduce the impact of DC faults is also studied. Enhancement of short-term frequency stability under high RE penetration using BESS is demonstrated by Talaq et al. [15]. Some contemporary works also highlighted the methods for determining the optimal sizing of the BESS to allow high RE NSGS penetrations [16,17]. The effect of delays and ramp rate of BESS on frequency dynamics are analysed by Borgan et al. [18]. Although impressive progress has been made in analysing the impact of BESS on mitigating frequency stability risks, little has been reported to determine a method for evaluating the beneficial effects of BESS operations. Besides, no research has been reported which has presented a framework to allow for a systematic comparison between different BESS operating parameters (such as capacity and droop coefficient). Evaluation across multiple BESS capacities and droop settings, which allow for the direct comparison of BESS performance, is currently missing in the literature. Such a systematic understanding of BESS impacts on system frequency performance is likely to become important, with required BESS settings expected to evolve as power system operators look to improve their utilisation of the fast frequency response capabilities of BESS. For example, the minimum droop setting for Distributed Energy Resources (DER) has been changed by AEMO from 1.7% to 0.7% [19]. Thus, a comprehensive analysis to evaluate the frequency performance with multiple BESS capacities operating with multiple droop settings is relevant. Development of a methodology for directly comparing the ameliorating effect of BESSs for future power system planning is desirable.

This paper investigates how BESSs can enhance the frequency stability in future power systems with high RE NSGS penetrations. As a test case, the Queensland (QLD)–New South Wales Interconnection (QNI) separation event, which occurred on 25 August 2018, [20] was chosen. The inadequacies of current SG-based PFC for mitigating future frequency stability risks are highlighted, and the requirements of BESS in PFC for such future scenarios are analysed.

The main contributions of this paper are summarised as follows:

1. It has been demonstrated that the current primary frequency control arrangements by synchronous generators will not be adequate for future power system scenarios with high RE NSGS penetrations. Simulation studies show that if additional measures are not taken for PFC arrangements, QLD will be more vulnerable to over-frequency events for a similar contingency event as that which occurred in 2018 [20];
2. In response to the potential frequency stability challenges caused by low inertia systems due to high levels of NSGS RE integrations in QLD, the role of BESSs in PFC is studied in detail. Simulation results confirm that BESS, if suitably deployed, is capable of effectively managing the potential frequency stability risks under high renewable energy penetrations in QLD;
3. An iterative approach to analyse the impact of BESS capacity and droop settings on the frequency dynamics of a low inertia power system is introduced in this work. A variety of BESS capacities and droop settings were trialled, which demonstrated consistency in performance and the occurrence of diminishing returns. While rate of change of frequency and frequency nadir was improved with aggressive droop values and higher BESS capacities, limits were identified where further increments produce negligible impact. Simulation results demonstrate that droop-controlled BESS, with a capacity of nearly 17% of total system load, could avoid over-frequency generation shedding (OFGS) when the power system operates at 80% RE-based NSGS penetrations.

The remainder of the paper is organised as follows. The NEM grid requirements and PFC in power systems with high RE penetrations are described in Section 2. In addition, the droop controller implementation for BESS is discussed. Section 3 details the QLD separation event and presents and validates the power system model used in this study. In Section 4, the impact of droop-controlled BESS in primary frequency control of power systems with different levels of renewable energy penetrations are analysed by extensive simulation studies. Finally, conclusions are presented in Section 5.

2. Frequency Control in Power Systems with High RE Penetration

2.1. Frequency Control and Grid Requirements

There are several stages of frequency response following a power imbalance resulting from a contingency event: the inertial response to regulate the Rate-Of-Change Of Frequency (ROCOF; uncontrolled response), PFC, secondary frequency control, and tertiary frequency control. Immediately after a contingency event occurs, SGs connected to the network either reduce or increase their speed, and thus the quantity of stored energy associated with their rotating mass [20], with simultaneous injection or consumption of power to/from the network, respectively. This response is known as an inertial response and is automatic. The total initial injection or consumption of power is exactly equivalent to the difference in supply and demand that has arisen. The inertial response of the system is both proportional to and the determinant of the ROCOF. This inertial response typically lasts for up to 10 s, depending upon system characteristics and the subsequent speed of PFC action [21]. Once this initial frequency/generator speed variation has occurred, preliminary action is taken by the governor and turbine of PFC-enabled SGs, with their input reference altered according to frequency deviation. PFC stabilises the frequency to a new steady-state point over a period of typically 0–30 s [22]. After this critical stabilisation occurs, secondary and tertiary control first recovers frequency to within the normal operating bounds and then re-balances generation between regions if required. This typically takes place for a duration of 30 s–30 min [22]. This paper only concentrates on BESSs providing PFC.

The ROCOF ($\dot{\Delta f}$) for a power system with supply-demand imbalance can be realised by the swing Equation [22]:

$$\dot{\Delta f}\frac{2H_{sys}}{f_0} = \frac{(P_g - P_e)}{S_{sys}} \quad (1)$$

where f_0 is the nominal frequency of the system, P_g and P_e are the total mechanical input and electrical output power, respectively, and S_{sys} is the base electrical power rating of the system. The aggregate inertia constant of the system is represented by H_{sys}. The inertia constant of a single synchronous machine, meanwhile, is defined by Kundur et al. [22] as:

$$H = \frac{E_{k_{stored}}}{S_{rated}} = \frac{1}{2} \times \frac{J\,\omega^2}{S_{rated}} \tag{2}$$

where $E_{k_{stored}}$ is the stored kinetic energy of a synchronous machine rotor with the rotational speed ω, moment of inertia J, and nominal power rating S_{rated}.

The sum of stored energy in rotating masses of all connected SGs is the equivalent or aggregate inertia of the system. In a power system, containing n generating units, the aggregate system inertia constant H_{sys} is obtained from:

$$H_{sys} = \frac{\sum_{m=1}^{n} H_m \times S_m}{S_{sys}} \tag{3}$$

where H_m and S_m are the inertia constant and the nominal power of the mth unit, respectively.

The system inertia decreases when RE NSGSs replace SGs. According to Equation (1), ROCOF ($\dot{\Delta f}$) is inversely related to the system inertia. This implies that frequency will deviate more rapidly (higher ROCOF) if an unexpected change occurs in a lower inertia system. A higher ROCOF, if sustained, can trigger protection relays and may cause the cascaded tripping of generators [23]. Higher initial ROCOF may contribute to a large frequency deviation, which can also cause generator tripping and load shedding [23]. The need for generators (or other elements of the power system) to provide PFC, and in particular fast-acting PFC, becomes more acute as system inertia is further reduced.

The change in power output of a PFC-enabled generator P_m as a function of system frequency deviation Δf is known as its speed-droop characteristics or speed-governor characteristics, as shown in Figure 1. The well-established method of frequency control is called droop control [22].

The relationship between change in generator output power and frequency deviation can be represented by R_m, and is defined as follows [22]:

$$R_m = -\frac{\Delta f}{f_0} / \frac{\Delta P_m}{S_m} \tag{4}$$

At the system level, the power-frequency characteristic κ is given by Equation (5), which determines the steady-state frequency error after PFC has restored the system balance [22].

$$\kappa = -\frac{\Delta P}{\Delta f_{ss}} = \sum_{m=1}^{n} \frac{1}{R_m} \times \frac{S_m}{f_0} \tag{5}$$

where Δf_{ss} is the steady-state frequency difference from the nominal frequency f_0, with the range of the active power demand ΔP, and R_m is the droop or regulation.

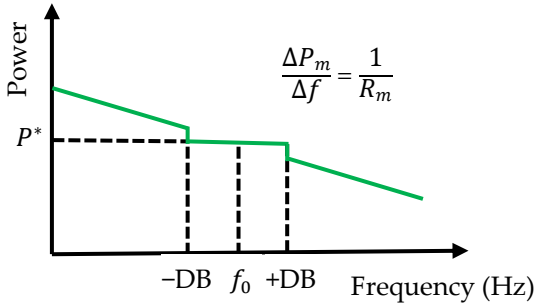

Figure 1. Typical power–frequency droop characteristic.

The power-frequency characteristics provide the fundamental estimation of the frequency response in an electrical power system following an imbalance between generation and load.

In Australia, the recommended setting for ROCOF is $\leq$0.5 Hz/s [24]. Generator dispatch should be arranged so that ROCOF would not exceed this value for a worst-case foreseeable contingency event. However, each state of Australia has different inertia constraints because of distinct levels of RE penetration [24]. For example, in the state of Tasmania, a limit of 1.18 Hz/s is applied when frequency drops below 49.0 Hz. Figure 2 shows the frequency operating standards (FOS) for the mainland NEM. OFGS and under-frequency load shedding (UFLS) occur between 51–52 Hz and 47–49 Hz, respectively [25,26].

With decreasing inertia in the system as NSGSs replace SGs in future, an event similar to the QNI separation described earlier could result in high frequency deviation, leading to cascading failures and power system blackouts. To avoid such an outcome and manage low inertia systems will require appropriate frequency support from NSGSs and other non-conventional elements. BESSs could be of great help because they are capable of providing fast frequency response [18,21,27].

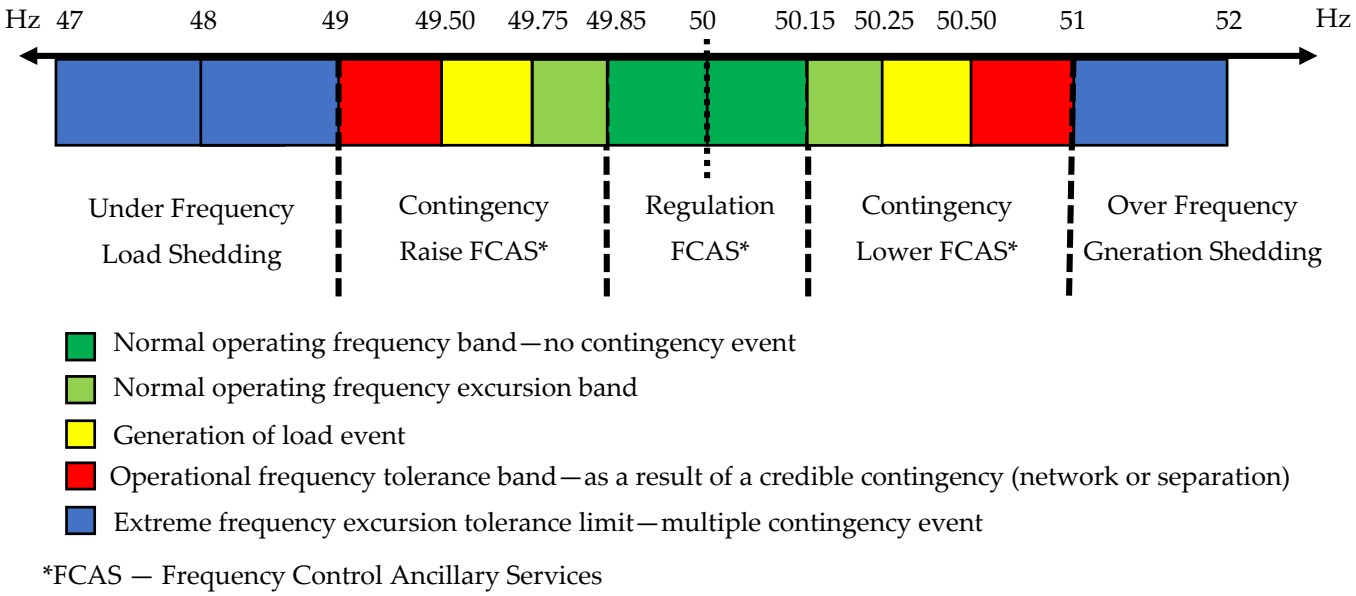

Figure 2. Frequency operating standards—Mainland National Electricity Market (NEM) [26].

2.2. PFC Using BESS

BESS control systems control the power flow between the BESS and the electrical grid via a voltage source converter (VSC). The measurements of voltage and frequency, which are used by the control systems, are taken locally. In order to provide primary frequency control, the BESS regulates active power output with the total power output restricted by BESS and converter capacities S_{BESS}, as shown in Figure 3. The power adjusted by the BESS into the electrical network due to PFC contribution, Δp_{PFC}, is given by:

$$dP_{BESS} = S_{BESS} \left(\Delta p_{PFC} + P^* \right) \quad (6)$$

where BESS power rating and pre-set output power are represented by S_{BESS} and P^*, respectively.

In Figure 3, Δf (pu) is the frequency deviation resulting from a supply–demand imbalance event and computed as the difference between the nominal system frequency, f_0, and the grid frequency, f. R_{BESS} represents the droop coefficient of the BESS inverter in pu. A dead-band is employed to ensure that the PFC response is only activated if the actual

frequency differs by ±150 MHz (±0.003 pu) from the nominal value [26], corresponding to the normal operating frequency band in the Australian NEM.

The ramp rate of a BESS has a significant influence on the effectiveness of PFC, with a fast response required to mitigate the impact of high ROCOF in a system. Several authors have addressed the issues related to BESS ramp rate in order to assess the ability of BESS to provide fast frequency response [18,21,27]. A test survey of the National Renewable Energy Laboratory (NREL) for a 1 MW/1 MWh battery system (SMA inverter, LG Li-ion batteries, step-up transformer) demonstrated a very fast response time (20–40 ms) of BESSs in both grid-forming and grid-following modes of operation [27]. In this paper, we apply a ramp-rate of 1 pu/20 ms, thus representing the state-of-the-art battery response capabilities.

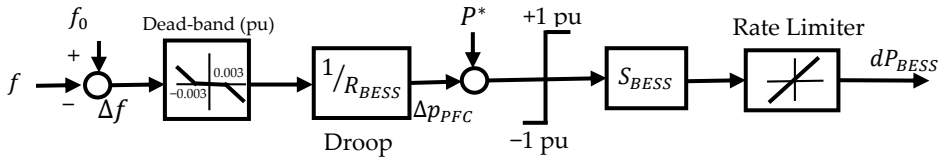

Figure 3. Block diagram of the implementation primary frequency control (PFC) using a battery energy storage system (BESS).

3. Lumped System Model and Separation Event Validation

This section describes the QNI separation event of 2018 [28] and the lumped generator system model, which we used to replicate the event via simulation. The QLD power network is connected to the rest of the NEM via QNI [28]. At the time of separation, which occurred as a result of transmission line faults associated with a lightning strike, QNI was exporting nearly 857 MW from QLD to the rest of the Australian system, representing approximately 12% of total QLD generation. The separation event resulted in QLD system frequency first rising to 50.9 Hz before settling at 50.6 Hz. At the time of separation, the generation mix in QLD was dominated by thermal coal-based SGs, with these being able to deliver adequate primary frequency response to stabilise frequency. However, future scenarios will see far less SG available for providing PFC (AEMO expects to achieve on average 80% of RE NSGSs in QLD by 2040 [29]), and thus a separation or similar contingency event such as this may result in larger frequency under/overshoot, higher ROCOF, longer settling time, and larger frequency deviation after stabilisation. Unless frequency response is provided from other sources, this could potentially lead to UFLS/OFGS or power system blackout.

The simplified power system model used to represent the QLD system and simulate the separation event is shown in Figure 4. The system includes two lumped SGs, SG1 and SG2, representing the total synchronous generation of QLD, and RE-based NSGS representing solar and wind generators. Because we considered system frequency response only in this study, and because frequency deviations propagate across the transmission network on a much smaller timescale than frequency responses of SGs, we can consider that all generators in the system were exposed to identical frequency. Hence, we can justify the use of a single-node, or copper-plate, lumped-generator approach for these studies.

During the separation event, QLD had 7490 MW of synchronous generation capacity connected to the system [28]. Two factors are considered for determining the capacity of SG1 and SG2, primary frequency reserve [29] and minimum generation level [29]. The fleet of QLD SGs are reported to have a minimum generation level between 26% and 40% [29]. In this study, an average minimum generation level P_{min} of 33% is chosen. The minimum regional reserve requirement for the QLD system is stated by the system operated as 666 MW [29]. By considering this minimum reserve, for both frequency raise and lower requirements, the capacity of SG1 (PFC enabled) and a suitable initial load were computed. The following relationship was utilised to calculate the SG1 capacity:

$$\text{SG1} = \frac{2 \times MRL}{(1 - P_{min})} \tag{7}$$

where *MRL* represents the minimum reserve level of the QLD system.

The remainder of the generation capacity and generation output at the time of the event was allocated to SG2, which was not enabled for PFC. The inertia for SG1 and SG2 were proportionally calculated from the total QLD system inertia, based on their respective generation capacities. The generation capacities and outputs for the system model at the time of separation are summarised in Table 1.

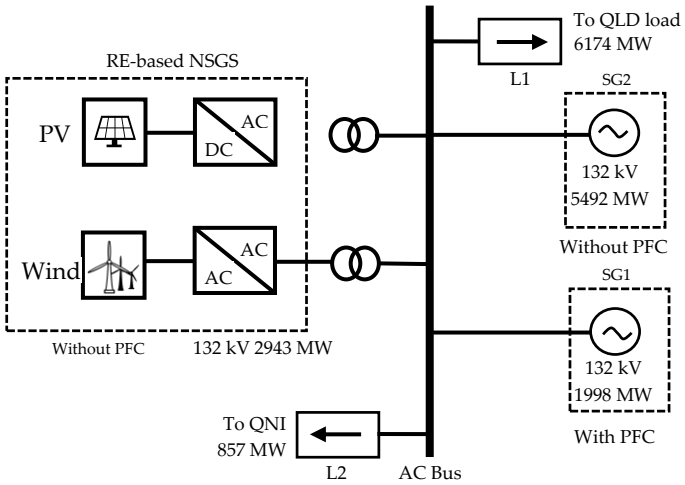

Figure 4. A simplified power system model with two lumped SGs and non-synchronous generating sources (NSGSs), representing the Queensland (QLD) power system. PFC—Primary Frequency Control.

Table 1. Generation parameters of the modelled QLD power system during the separation event [28].

SG1 (PFC)		SG2		SG Total		Total RE NSGS		% of Total RE
Capacity (MW)	Output (MW)	Capacity (MW)	Output (MW)	Capacity (MW)	Output (MW)	Capacity (MW)	Output (MW)	18.9%
1998	1332	5492	4368	7490	5700	2943	1331	

The total load of the QLD power system immediately prior to the separation event was equal to 7031 MW, which we represent by two components: L1 = 6174 MW, the local QLD load; and L2 = 857 MW, the power exported by QNI. The separation event was modelled by removing the load L2 from the system, resulting in 857 MW of excess generation in QLD. After the separation event, there was a sustained aggregate reduction in synchronous generation output of around 600 MW, as shown in Figure 5. The curtailment of solar PV contributed to the additional 257 MW generation reduction required to restore system balance [28].

In this study, we used our power system model to investigate the PFC response from SGs and RE NSGS in the QLD power system after the separation event and under a range of future scenarios. For this purpose, simplified mathematical models of a conventional governor and turbine were used, representing conventional synchronous generator frequency control, and described by Amin et al. [11]. The inertia is defined as stored kinetic energy in watt-second ($\frac{1}{2} J\ \omega^2$); in the QLD power system it was 26,800 MWs at the time of separation [24]. This value was provided by synchronous generators of Queensland (the total capacity of 7490 MW, the inertia constant was determined calculated using Equation (2) as 3.58 s). The droop constant applied to SG1 for simulations corresponded to the final steady-state frequency error observed after the separation event, with this value also retained for all subsequent simulations [28]. Figure 5 shows the measured and modelled QLD system frequency and SG active power output during the QNI separation event. It can be observed that the initial ROCOF is nearly identical, also shown in Table 2, confirming

that both the simulated system and the actual system had the same total system inertia. The remainder of the response generally matches well too, with the only major difference being in how quickly frequency returns from the zenith value to its final steady-state value. Close inspection of the published measured data from the separation reveals a variety of both delay in response and ramp rates of individual SGs, as well as quite varied behaviours of different PV curtailment schemes in operation. It is of course not possible to include all these different individual generator response behaviours in a lumped model approach, and therefore the dynamic response of our model is different in this respect from the original QLD observations. In particular, there are insufficient data available to allow precise modelling of the curtailment response of operating PV systems, which varied considerably among different plants connected at the time. Hence, our model, which uses a simplified PV system response, yields this minor difference in frequency response when compared to the observed system. Nonetheless, the comparison demonstrates that both our simulation and the actual system have the same frequency overshoot, steady-state frequency, and change in synchronous generation output. This result gives confidence that the model can be used to reliably characterise the response to such an event under the different conditions investigated in the remainder of this paper, with similar minor variations in response to be expected between simulations and a corresponding practically deployed system.

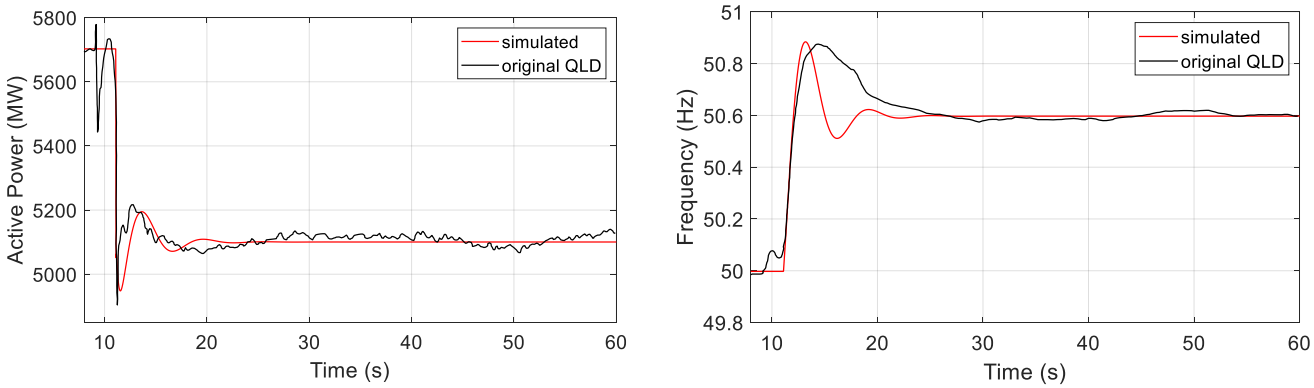

(**a**) (**b**)

Figure 5. (**a**) Active power response of SGs and (**b**) frequency response of QLD power system.

Table 2. Rate-of-change of frequency (ROCOF) and frequency zenith comparison

Model	ROCOF (Hz/s)	Frequency Zenith (Hz)
Original QLD	0.458	50.90
Simulated	0.456	50.88

4. Simulation Results and Discussion

This section discusses the simulation results under different simulation case studies which are organised into four groups, as follows:

- Group A demonstrates the impact of RE NSGS penetration on PFC, when RE replaces conventional SGs;
- Group B investigates the effect of utilising a single BESS with different droop coefficients, along with SGs, for PFC response;
- Group C shows the impact of utilising a fixed droop coefficient with different BESS capacities, along with SGs, for PFC response;
- Group D investigates PFC response using a single BESS capacity with different droop coefficients, with SGs now excluded from providing PFC response.

Frequency stability is examined based on the NEM FOS under different levels of RE NSGS penetrations. Case studies of Groups B–D show the impact of BESS for mitigating increasing RE NSGSs penetrations. The power system model used in Groups B–D case studies is shown in Figure 6 (two SGs, BESS-inverter and RE based NSGSs), with SG parameters consistent with the validation presented in the proceeding section.

The observed response of solar PV, which included partial curtailment from some operating plants, was not taken into account in these studies. The response from each respective PV system, which can be considered as over-frequency curtailment only rather than PFC, is not clearly defined at this stage and cannot easily be modelled. The authors recognise that solar PV may potentially provide PFC in future power systems with high PV penetration; however, this paper focuses on investigating the impact of using BESS over SGs for PFC in low inertia power systems.

In the observed system, QLD SGs provided a 600 MW primary frequency response. Therefore, in the simulation model, a switchable load L2 = 600 MW was used to represent the QNI export quantity that SG and/or BESS PFC must respond to.

This demonstrates that both the simulated system and the actual system have the same initial ROCOF and steady-state frequency.

For all cases, such as the QNI separation, a decreased step-load of L2 = 600 MW was used to analyse the performance of primary frequency response by observing ROCOF, frequency zenith, and frequency settling time. A 400 ms window was considered to measure the ROCOF [30–32]. BESS degradation costs and installation costs were excluded, because the main objective of this paper was to analyse the impact of BESSs in PFC.

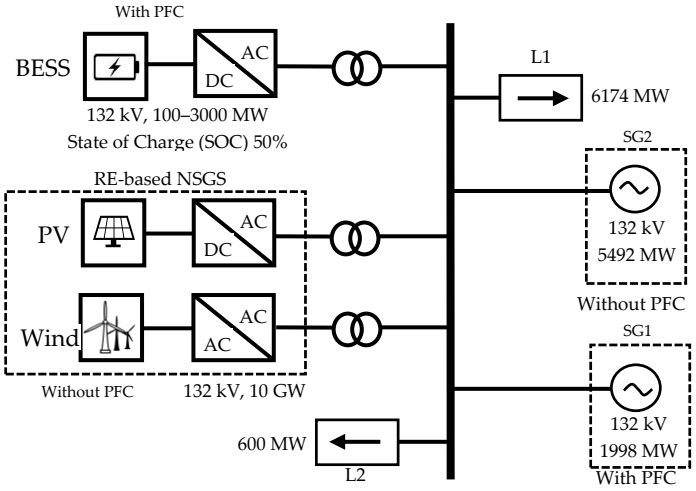

Figure 6. Power system model consisting of two SGs, BESS-inverter and an RE-based NSGS.

4.1. Group A: Different Levels of RE NSGS Penetration

The aim of the case studies in Group A was to investigate the impact of different levels of RE NSGS penetrations on PFC. During the separation event, QLD had RE NSGS penetrations of 18.9%. However, according to the ISP 2020 report [2], by 2040, the approximate scale of RE NSGS penetration in QLD power system will increase and reach up to 80% [2,8]. Therefore, case studies undertaken in Group A considered high RE penetration. Results are presented in Table 3.

RE NSGSs are expected to replace conventional SGs. Therefore, in our simulation, the increasing RE NSGSs penetration was simulated by decreasing the installed capacity of SG2. At the same time, the level of SG1 was unchanged to ensure the required minimum reserve level of the QLD system.

Table 3. Parameters for Group A case studies.

Case Description		A40—40% RE	A60—60% RE	A80—80% RE
Total RE as percentage of Total QLD Generation		40% RE	60% RE	80% RE
SG1 (PFC)	Capacity (MW)	1998	1998	1998
	Output (MW)	1332	1332	1332
SG2	Capacity (MW)	3629	1861	93
	Output (MW)	2886	1480	74
SG Total	Capacity (MW)	5627	3859	2091
	Output (MW)	4218	2812	1406
RE NSGS output (MW)		2812	4218	5625
System Inertia (MWs)		20,134	13,808	7482

Figure 7 shows the frequency response of the system under different levels of RE penetration. For Case A40—40% RE NSGS penetrations, the red line indicates the primary frequency response, provided by SG1, when the step-load L2 = 600 MW was dropped out from the system. This 40% RE penetration (2812 MW) caused a reduction in total system inertia by approximately 25%. This causes a reduced capability to provide an inertial response to the system, thus resulting in an increasing ROCOF following the event. The ROCOF increased by nearly 25% compared to the actual separation event, where 18.9% RE penetration occurred (as shown in Table 4). The damping capability of the system decreased, which caused increasing oscillations in the system. Therefore, the duration of energy exchange between the rotating mass of SGs and electrical network increased. Although the primary frequency reserve provided by SG1 remained unchanged, frequency settling time increased. Frequency zenith was reached at the OFGS limit while the ROCOF level was still under the acceptable range. The delayed primary response of SG1 could not arrest the increasing ROCOF after the initial inertial response to the system. Therefore, a fast frequency control support would be needed.

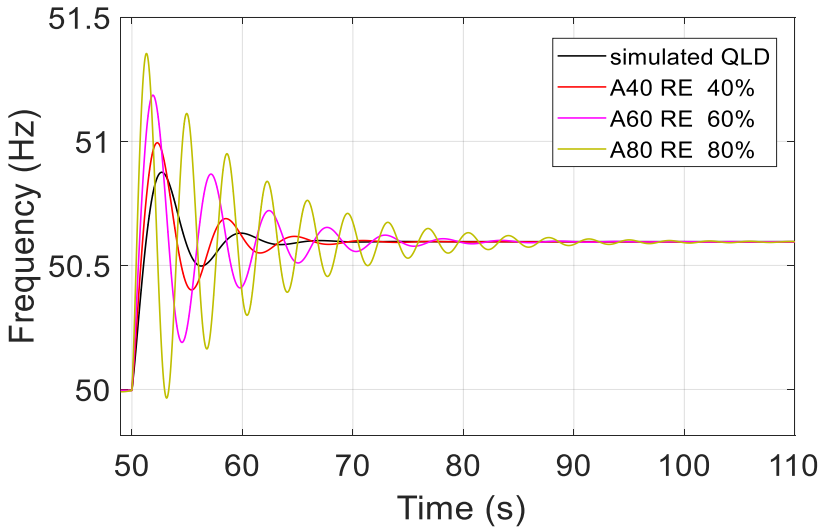

Figure 7. Frequency response of the system under different levels of RE penetration.

Table 4. ROCOF and frequency zenith for Group A case studies.

Cases A	ROCOF (Hz/s)	Frequency Zenith (Hz)
A40—40% RE	0.653	51.00
A60—60% RE	0.825	51.19
A80—80% RE	1.325	51.35

With the 60% RE NSGSs penetrations, the frequency zenith exceeded the OFGS limit of 51 Hz, set by NEM [25]. ROCOF increased by nearly 60% because of the 50% reduction in inertia of the system, as shown in Table 4. Furthermore, with the 80% RE NSGSs penetrations, the total inertia of the system dropped by 75%, thus resulting in increased ROCOF and frequency settling time by 75% and 65%, respectively, compared to the actual separation event. Frequency zenith reached 51.35 Hz, which is 0.35 Hz higher than NEM OFGS limit.

The simulation results show that the PFC provided by the existing conventional SGs may not be sufficient to provide enough of a PFC response for stabilising the frequency and minimising increasing ROCOF and frequency zenith, following a contingency event. Therefore, the current arrangements of PFC need to be modified, as suggested by AEMO [33]. The issue of managing the risk of frequency instability in low inertia power systems using BESSs is considered below.

4.2. Group B: Fixed BESS Capacity with Different Droop Characterstics

Case studies in Group B were designed to investigate the impact of utilising a single BESS with different droop coefficients. The NEM expect to achieve 80% RE penetrations by 2040 in QLD [2]; therefore, 80% RE NSGS was selected for the Group B case studies. Considering the current trends in BESS installation in Australia, in our paper, we assumed BESSs of different capacities [2]. In Group B, a single BESS of 500 MW was used for simulation. The droop coefficients and BESS capacity used for Group B case studies are shown in Table 5.

Table 5. Group B, different droop coefficient, fixed BESS capacity, A80—80% RE penetration.

Cases B	BESS Capacity (MW)	Droop Coefficient ($^1/_{R_{BESS}}$)
B80a—80%RE	500	50
B80b—80%RE	500	100
B80c—80%RE	500	150
B80d—80%RE	500	200
B80e—80%RE	500	300

Figure 8 shows the frequency response of the system when BESSs are used. Droop-controlled BESS provide an extra response by increasing absorption active power when the load of 600 MW is disconnected, as shown in Figure 6. The steady-state frequency is improved. Unlike SGs, BESS-inverter control systems do not cause any delay in response to the contingency.

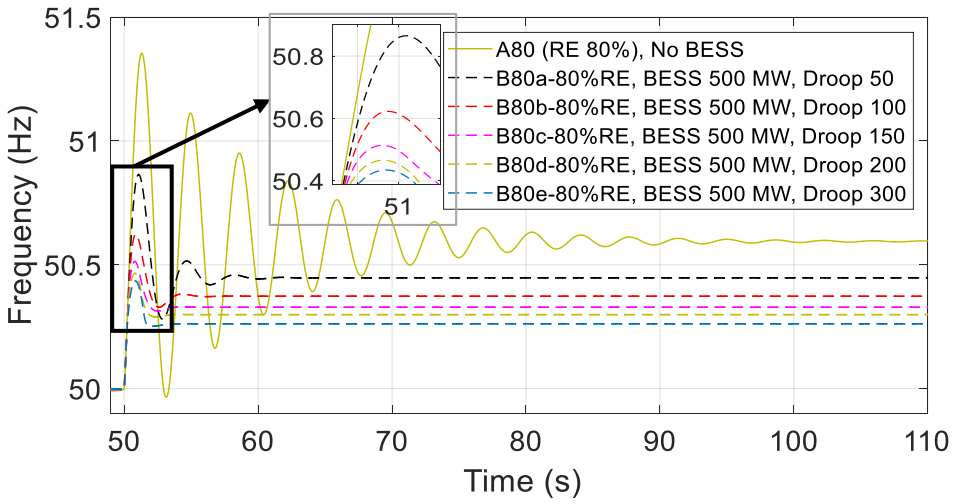

Figure 8. Frequency response of the system without and with BESS, and different droop coefficients.

A high droop coefficient enhances the BESS response in providing the additional damping to the system, which results in decreasing the ROCOF, as shown in Figure 9. The additional damping provided by droop-controlled BESS works as a shock absorber, lowering the frequency zenith by approximately 0.90 Hz while reducing oscillations by nearly 90%, as shown in Table 6. With a 500 MW BESS, when droop coefficient is increased by 80%, the frequency zenith is decreased by nearly 1%.

Table 6. ROCOF and frequency zenith for Group B.

Cases B	ROCOF (Hz/s)	Frequency Zenith (Hz)
B80a—80%RE	1.208	50.86
B80b—80%RE	1.118	50.62
B80c—80%RE	1.043	50.51
B80d—80%RE	0.978	50.47
B80e—80%RE	0.888	50.43

An aggressive droop value or high droop coefficient can result in a saturation effect, owing to BESS output reaching its full capacity (maximum allowable charge rate in this case). Thus, a BESS of low capacity cannot change its output power any further, and additional damping cannot be provided to the system. However, BESSs with high droop coefficient can play a key role in reducing frequency oscillation. Therefore, high-capacity BESSs with a high droop coefficient may be required for providing PFC in power systems with high NSGS RE penetrations. In Group C, BESSs of different capacities with a fixed droop coefficient were used to provide PFC in a power system with 80% RE penetration. As shown in Figure 8, for a BESS of 500 MW, an increment in the droop coefficient from 200 (Case B80d) to 300 (Case B80e) does not decrease the frequency zenith significantly (0.04 Hz). This is because the BESS output enters saturation, reaching its frequency reserve capacity limit, as shown in Figure 9.

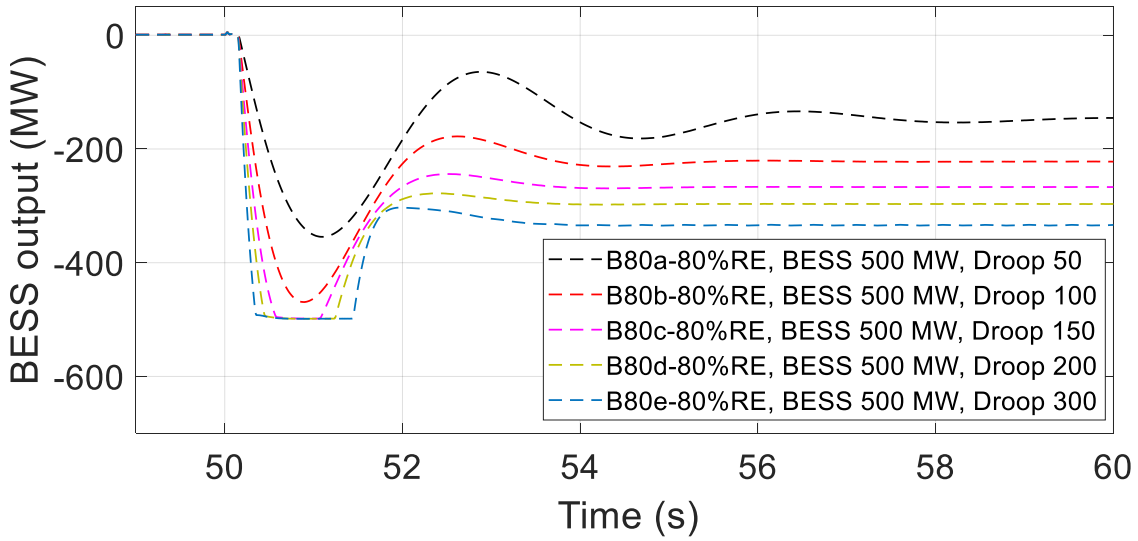

Figure 9. 500 MW BESS output power under different droop coefficients when 80% RE penetration occurs.

4.3. Group C: Fixed Droop Characteristic with Different BESS Capacity

In Group C, the capacity of the BESS was varied with a fixed droop coefficient of 300, as shown in Table 7 (the maximum BESS capacity is limited to 3 GW). AEMO expects to achieve nearly 3 GW of storage in the QLD power system by 2040 [2].

Table 7. Group C, different BESS capacity, fixed droop coefficient, A80—80% RE penetration.

Cases C	BESS Capacity (MW)	Droop Coefficient ($^1/_{R_{BESS}}$)
C80a—80%RE	1000	300
C80b—80%RE	2000	300
C80c—80%RE	3000	300

As shown in Figure 10, the frequency zenith decreases with the increase in capacity of BESS. Increased capacity of BESS with high droop coefficient provides additional damping to the system effectively, with a decreasing frequency oscillation and frequency settling time. When a BESS of 1000 MW with 300 droop coefficient provides the PFC, the frequency zenith is 50.28 Hz. The frequency zenith is decreased to 50.22 Hz with a BESS of 2000 MW and a droop coefficient of 300, as shown in Table 8. However, when the BESS capacity is increased from 2000 MW to 3000 MW, the frequency zenith is decreased by 0.02 Hz. The lesser improvement in frequency zenith can be explained by the fact that the droop coefficient remains unchanged (300) while capacity of the BESS was increased, but output power was constrained by frequency dead-band and ramp rate, as shown in Figure 11. Therefore, it can be deduced that the droop coefficient of BESS plays a substantial role in frequency control.

Table 8. ROCOF and frequency zenith for Group C.

Cases C	ROCOF (Hz/s)	Frequency Zenith (Hz)
C80a—80%RE	0.694	50.28
C80b—80%RE	0.554	50.22
C80c—80%RE	0.497	50.20

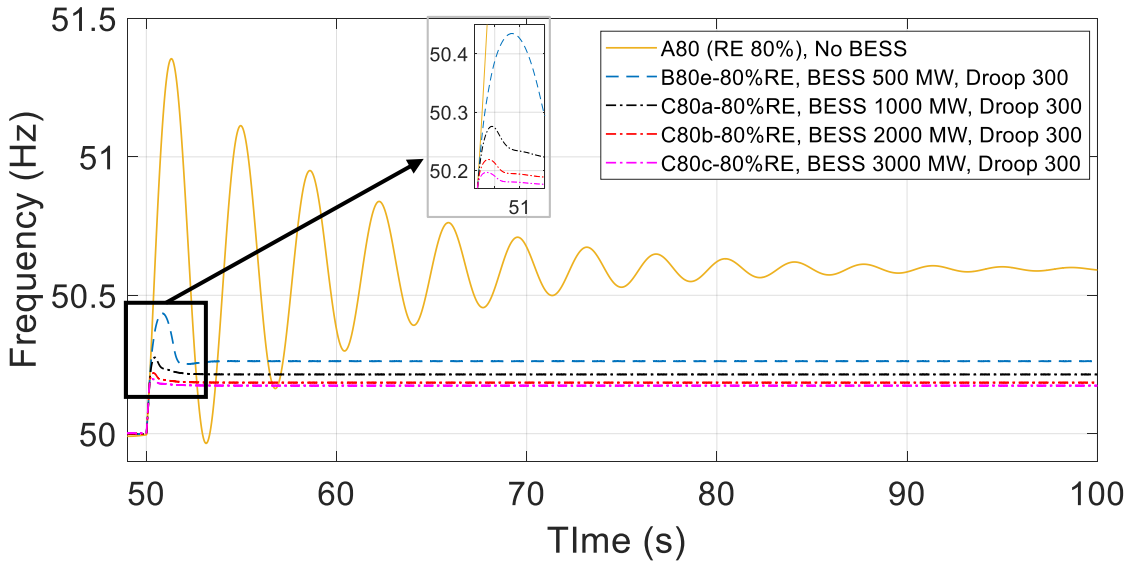

Figure 10. Frequency response of the system when different BESS capacities provide PFC using a fixed droop coefficient under an 80% RE penetration scenario.

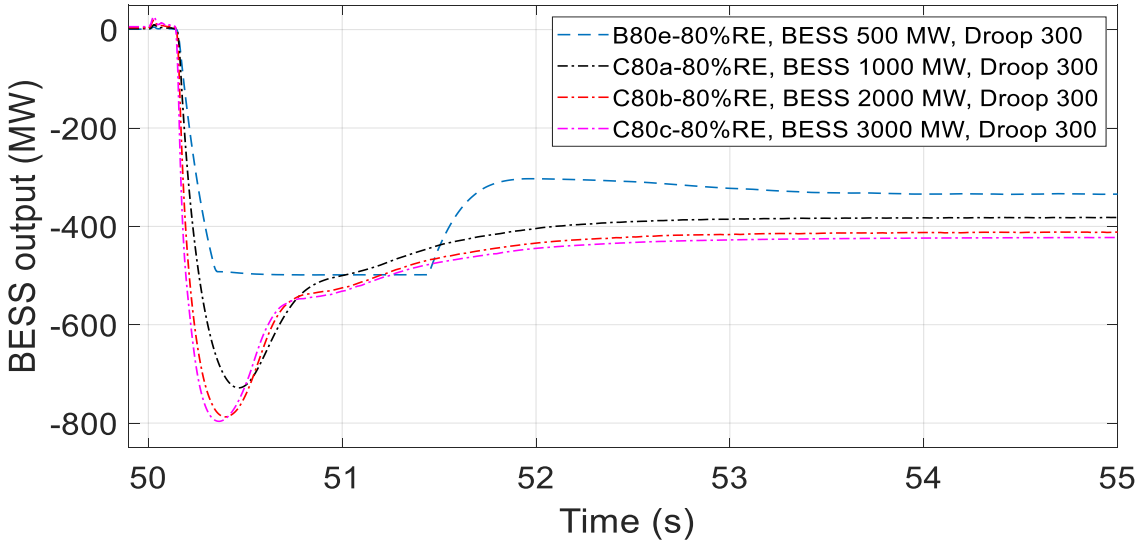

Figure 11. BESS output power with a variation in BESS capacities.

To further examine the impact of the capacity of BESSs and droop coefficient on PFC, 22 different values of droop coefficient, and 22 different capacities of BESS were investigated. This method was applied for demonstrating the comparison of the capacity of BESS with varying characteristics of droop. As depicted in Figure 12a, frequency settling time decreases with the increasing capacity of BESS and droop coefficient. However, for a lower capacity of BESS, when droop coefficient exceeds a critical value, a changing relationship between droop coefficient and frequency settling time can be observed. For example, as shown in Figure 12a, 100 MW BESS with a droop coefficient of 1000 increases the frequency settling time by approximately 50% compared to 100 MW BESS with a droop coefficient of 10. This is because a higher droop coefficient causes the low-capacity BESS output power to saturate to its full capacity for the same event. The fast response of BESS contributes to absorbing excess energy, which causes an increase in frequency oscillations, and results in undamped frequency response and longer frequency settling times. The frequency settling time decreases when the capacity of BESS increases. This is because the capability of absorbing excess power of the system increases. As a result, oscillation decreases with increasing the BESS capacity, as shown in Figure 9. Therefore, BESS cannot provide any additional damping to the system. However, for higher droop coefficients (higher than 110), a further increase in BESS capacity causes a significant decrease in the frequency settling time.

Figure 12b shows the effect of different capacities of BESS and droop coefficients on steady-state frequency. As shown in Figure 8, frequency settled at the level of 50.6 Hz, when only SGs provided PFC. As expected, when the contribution from BESS in PFC was enabled, the steady-state frequency reduced with the increase in capacity of BESS up to a droop coefficient of 90. For a lower capacity of BESS, the frequency deviation reduced with an increase in droop coefficient, approximately up to a drop of 120. This is because a high droop coefficient caused low-capacity BESSs to reach their full frequency reserves capacity quickly. For example, a BESS of 100 MW reaches output saturation with a droop coefficient of 120 when a 600 MW step-decrease contingency occurs. The frequency settles at 50.4 Hz. However, any additional increase in droop coefficient from 120 does not improve the steady-state frequency significantly.

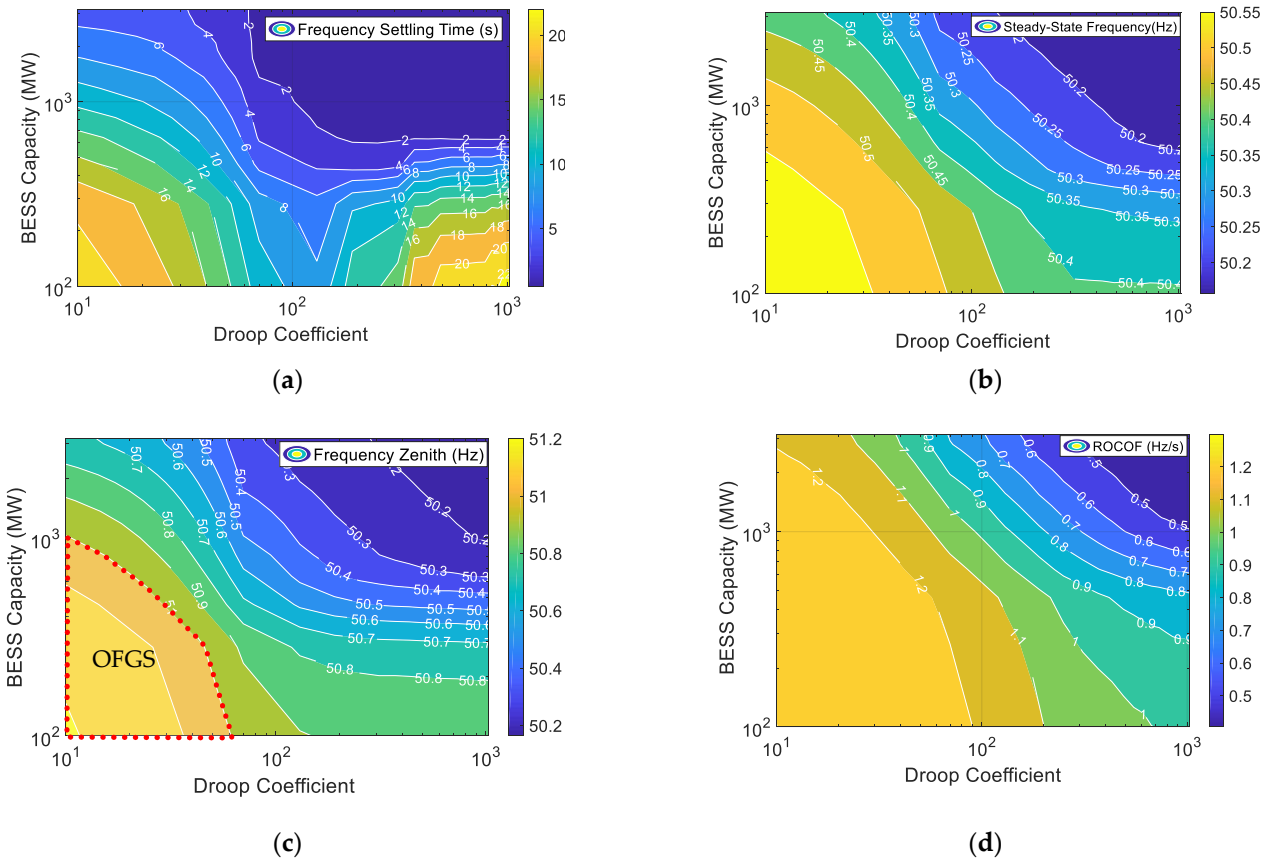

Figure 12. (**a**) Frequency settling time; (**b**) steady-state frequency; (**c**) frequency zenith; and (**d**) ROCOF for different capacities and droop coefficients of BESS, when both BESS and SG participate in PFC.

As shown in Figure 12c, frequency zenith was still beyond the NEM FOS requirements [26], when 100 MW BESS with low droop coefficients (below 60) were used. On the other hand, increasing the droop coefficient to a value of more than 60 resulted in a decreasing frequency zenith and avoiding the OFGS limit. Further increase in droop coefficients has a negligible effect on frequency zenith. This is because a high droop coefficient readily results in saturation for a BESS of low capacity, as mentioned previously, illustrated in the contour plots (Figure 12c), with frequency zenith showing little or no further reduction for an increased droop coefficient beyond a certain value for any given BESS capacity.

BESSs of low capacity with low droop coefficient had a less significant contribution in providing additional energy to the system and may not be sufficient for decreasing ROCOF. As indicated by Figure 12d, BESS output power response became limited by its maximum available ramp rate (chosen in accordance with the Li-ion BESS response time experimentally demonstrated by NREL described by Gevorgian et al. [27]). For example, when droop coefficient was higher than 600 for a BESS capacity of 3000 MW, there was no further reduction in ROCOF realisable, despite further increasing droop coefficient.

In summary, the results demonstrate that nearly 100 MW BESS with a droop coefficient of 60 would allow the QLD power system to avoid over-frequency events for a potential contingency such as the QNI separation.

4.4. Group D: Only BESS for PFC

Group D case studies were conducted to examine the impact of utilising different droop coefficients with a single capacity of BESS. Considering the contingency event of 600 MW and the minimum capacity of BESS found from the previous group of case studies, a single BESS of 1000 MW was considered for PFC in Group D case studies. This case

represents with the total anticipated capacity of BESS in QLD by 2030 [1]. Parameters for Group D case studies are listed in Table 9.

Table 9. Group D, different droop coefficient, fixed BESS capacity, no PFC from SGs.

Cases D	BESS Capacity (MW)	Droop Coefficient ($^1/_{R_{BESS}}$)
D80a—80%RE	1000	300
D80b—80%RE	1000	800
D80c—80%RE	1000	1300
D80d—80%RE	1000	1800

Figure 13 shows the frequency response of the system when a single BESS with different droop coefficients is used for PFC. Higher droop coefficients cause the BESS to respond aggressively, which enables it to be used for fast active power control. BESS can respond quickly and is driven to react fast due to the high droop coefficient; therefore, it can minimise the increasing frequency deviation faster than SGs. The frequency zenith decreases by 90% compared to Case A80—RE 80% by using a BESS capacity equal to 17% of the total system load. Because the BESS output ramp rate is limited to 1 pu/20 ms, further droop coefficient increment has less impact on decreasing the ROCOF and frequency zenith, as shown in Figure 13. The resultant frequency zenith and ROCOF listed in Table 10, confirm that with the increasing droop coefficient, ROCOF and frequency zenith decrease slightly. This is because the BESS response is limited by its ramp-rate [27]. Note that a dead-band of 150 MHz (currently implemented in Australia for PFC [33]) is applied the droop controller of the converter to ensure that only PFC is activated when the frequency deviation exceeds the NEM FOS limit.

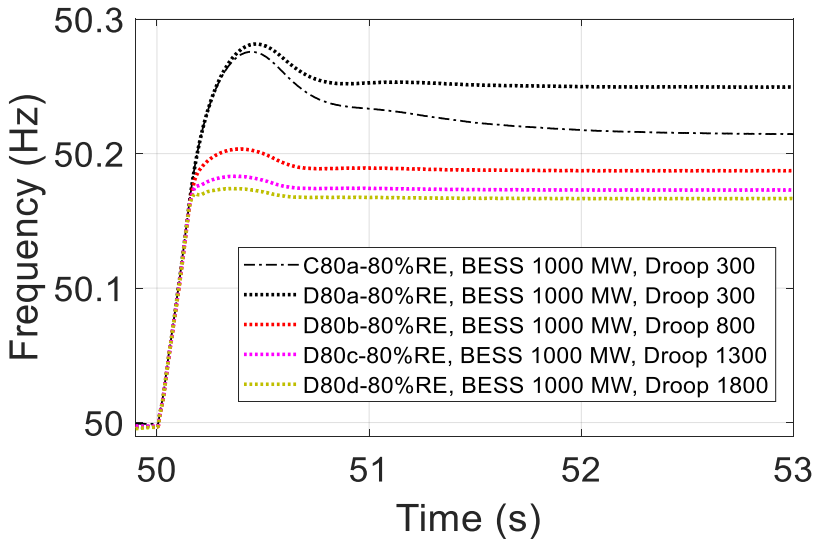

Figure 13. Frequency response of the system when a fixed BESS capacity provides PFC using different droop coefficients under an 80% RE penetration scenario.

As shown in Figure 14, the BESS output power increased up to 800 MW because of the use of a high droop coefficient. Fast increasing BESS output power supports the inertial response to the system that results in decreasing ROCOF, frequency zenith and oscillation. Frequency settling time was decreased by nearly 99% compared to A80—RE 80% (PFC provided by SGs). BESSs of low capacity (or equal to the event) may not be sufficient to provide PFC under NEM FOS requirements. Therefore, to enable power systems to operate securely, further investigations regarding the capacity of BESSs and droop coefficients are required.

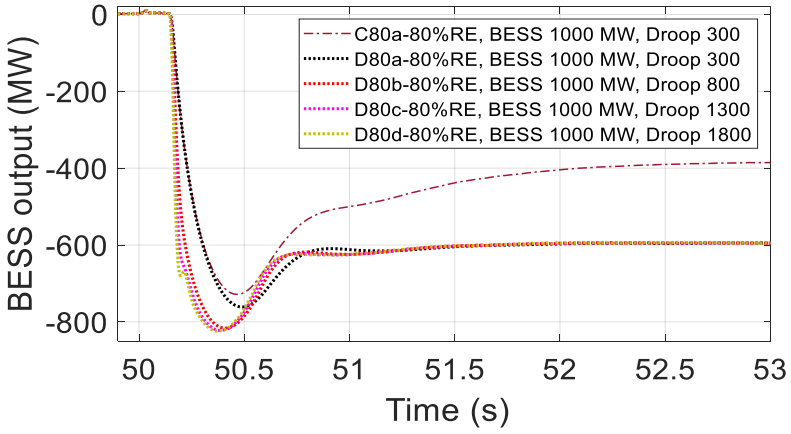

Figure 14. BESS output power under different droop coefficients when no PFC response is obtained from SGs.

Table 10. ROCOF and frequency zenith for Group D.

Cases D	ROCOF (Hz/s)	Frequency Zenith (Hz)
D80a—80%RE	0.703	50.28
D80b—80%RE	0.515	50.20
D80c—80%RE	0.464	50.18
D80d—80%RE	0.441	50.17

Figure 15a shows the frequency settling time for a range of BESS capacities from 600 MW to 3000 MW and droop coefficients from 10 to 1000 when only BESS was used for PFC. Frequency settling time increases with the increase in droop coefficient when a low capacity of BESS is employed. This is because high droop coefficients cause the low-capacity BESS to quickly provide its full capacity. Therefore, a high droop coefficient causes the low-capacity BESS output to become saturated, outputting its full capacity, for the same event. This fast but magnitude-limited response BESS output results in an under-damped frequency response and longer frequency settling times. However, the frequency settling time decreases and oscillations are reduced when the capacity of BESS is correspondingly increased. This illustrates the fact that high-capacity BESS increases the capability of quickly absorbing excess energy from the system. For example, a 1000 MW BESS capacity with 1000 droop coefficient decreased frequency settling time by 80%, as shown in Figure 15a, compared to when SGs provided PFC, illustrated in Figure 12a. As mentioned previously, a dead-band of 150 MHz was applied in the PFC. Therefore, a minimum 75 droop coefficient was required with a BESS of 600 MW to ensure the steady-state frequency under NEM FOS requirements, as shown in Figure 15b.

Steady-state frequency is improved by increasing droop coefficients. However, when droop coefficient reaches the value above 120, steady-state frequency does not improve significantly. Further increases in droop coefficients cannot increase BESS output power. BESS ramp rate constraints and dead-band in the PFC system of BESS-inverter restrict the additional increase in BESS output power, as shown in Figure 14. BESS with fast frequency response capability can settle the frequency faster than the cases where only SGs provide PFC, or PFC is provided by both an SG and BESS. Consequently, frequency oscillations decrease with an increase in the capacity of the BESS. Therefore, like steady-state frequency, frequency zenith has the same trends of improvements, shown in Figure 15c. ROCOF improves with the increase in both BESS capacity and droop coefficients, as shown in Figure 15d.

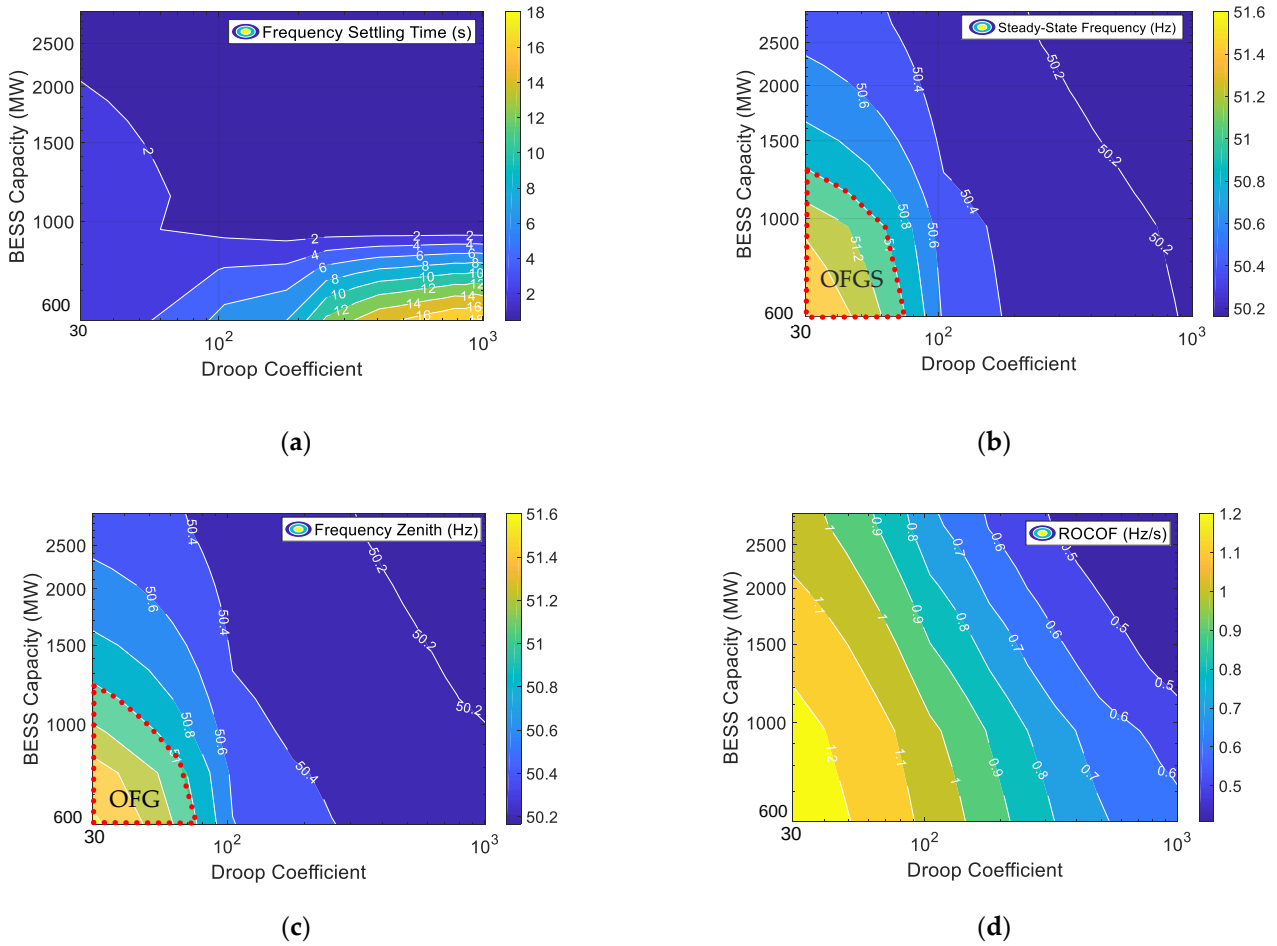

Figure 15. (**a**) Frequency settling time; (**b**) steady-state frequency; (**c**) frequency zenith; and (**d**) ROCOF for using different capacities and droop coefficients of BESS, when only BESS participates in PFC support.

In the future, the QLD power system is expected to consist of approximately 80% of generation from RE sources. In this case, the amount of required BESS will be significantly increased. To enable the QLD power system to operate securely under these circumstances (under NEM FOS, as shown in Figure 2), we demonstrate that approximately 800 MW BESS with a 1000 droop coefficient would be required.

4.5. Summary of Results

In this section, we summarise the major impacts that key BESS parameters have on system frequency response, based on our four groups of case studies for the QLD power system under future conditions with low contributions from SGs.

Simulation results of Group A depicted the frequency dynamics of the simplified QLD system under various levels of RE NSGS penetrations. As anticipated, with the decrease in system inertia associated with high levels of RE NSGS, the frequency response exhibited larger oscillations and faster ROCOF. It was found that the OFGS would be triggered at and above around 60% RE NSGS penetration. This study is intended to be beneficial in identifying the penetration limit which activates the OFGS. The study points to the fact that if additional measures are not in place with the increase in RE NSGS penetration level, QLD would be more vulnerable to over-frequency events for a similar separation event, and conversely would also be more vulnerable to under-frequency load-shedding for an equivalent contingency event triggering falling frequency.

The case studies for Group B were divided into several parts. Initially, the time-domain plots are presented which analyse the effect of droop coefficient setting for a particular capacity of BESS. This study is beneficial in discovering the impact of droop coefficient

setting on dynamic performance and damping characteristics of the system when BESS and SGs are both providing primary frequency response. As the droop value increases, the frequency performance is improved, as characterised by the frequency nadir and ROCOF. For a range of droop coefficients (50–300), it was shown that no undesirable oscillations can be observed. Subsequently it is demonstrated how BESS capacity influences the frequency behaviour of the system for a given droop. Simulation results showed that changing the capacity of BESS from 2 GW to 3 GW does not improve the frequency response significantly. This indicates that in order to utilise further increased BESS capacity and improve system frequency response, the droop coefficient should be correspondingly increased.

Finally, the effect of BESS capacity and droop coefficient on frequency dynamics are investigated for the case where the BESS provides the primary frequency response. This study can be beneficial to identify the possible BESS capacities and droop coefficients which would be suitable for managing the frequency stability risks under high RE NSGS penetration. For example, using a 1 GW BESS with a droop coefficient of 1000 could be a plausible option to satisfy the FOS limit of the NEM for QLD following a contingency event as described in this work. The study also analysed the ROCOF behaviour of the system, illustrating how it is possible to avoid BESS operating parameters which could aggravate frequency stability issues (higher ROCOF). For example, Figure 12c can be utilised to identify the range of droop coefficients and capacities of BESS which will not be able to manage the frequency stability risks and could activate OFGS (highlighted using a red dotted area). Additionally, this work can be used to identify the points beyond which an increasing capacity of BESS and droop coefficient might not be beneficial because performance improvement is negligible. Group D case studies show the frequency response when PFC is achieved only by BESS. Simulation results obtained in this group of case studies showed a similar trend as Group C, but with both reduced frequency zenith and reduced settling time, owing to the faster response that the BESS can provide.

5. Conclusions

This paper demonstrates, by re-creating via simulation an Australian power system separation event under scenarios with decreasing levels of inertia, that conventional SG retirements and their replacement with RE NSGS will deteriorate the frequency response in power systems. In Australia, a substantial RE NSGS penetration is anticipated in the generation mix in future, with wide-spread closures of coal-fired power generation stations expected by 2040. QLD represents a good example of future power systems where, by 2040, the anticipated generation mix will reduce the system inertia level by approximately 75%. This can potentially increase the system vulnerability to frequency violations following any unexpected load or generation events, as demonstrated by the simulation studies presented in this paper.

Simulation results also demonstrated that the ROCOF and frequency zenith are increased with withdrawals of SGs, even if the MRL is maintained by conventional SGs. It was found that an RE penetration of approximately 40% can cause the frequency zenith to reach the OFGS limit in QLD following a separation event such as that studied in this paper, currently the largest contingency event for which the system must be prepared. When 80% RE NSGSs penetration occurs, the total inertia of the system is reduced by 75%, resulting in increased ROCOF and frequency settling time by 75% and 65%, respectively, compared to the observed separation event (corresponding to 18% RE NSGS penetration). Frequency zenith was 51.35 Hz, 0.35 Hz higher than the NEM OFGS limit. As a measure to manage these potential frequency stability risks, different BESS capacities and droop characteristics are investigated, and their impact on the PFC in QLD power system model is analysed.

Simulation studies concluded that a BESS capacity equal to the 15% total generation capacity could limit the frequency zenith to below the OFGS boundary and improve frequency by 2% for a power system with 80% RE NSGS penetration. This investigation also shows that a high capacity of BESS with high droop coefficient can provide additional damping to the system, resulting in decreased frequency oscillation and frequency settling

time, and thus can help to manage frequency stability risks effectively. However, depending on the level of event and the frequency response characteristics of other PFC enabled sources, BESS with high droop coefficient and low capacity may not be sufficient to provide adequate damping to the system, which can cause a higher ROCOF and frequency deviation with extended frequency oscillations. Therefore, the capacity of BESS is a significant factor which needs to be considered for PFC applications as SG retirements increase in power systems. In future works, a framework to tune a suitable droop coefficient for BESS in power systems with low SG contributions and high RE penetration will be developed.

Author Contributions: Conceptualisation, methodology, software validation, formal analysis, and original draft preparation were done by M.R.A.; supervision and editing were carried out by M.N., E.F., K.S.A. and S.B.N. All authors have read and agreed to the published version of the manuscript.

Funding: This research received no external funding.

Institutional Review Board Statement: Not applicable.

Informed Consent Statement: Not applicable.

Acknowledgments: The authors would like to acknowledge the support provided by the Australian Renewable Energy Agency (ARENA) under contract number 2018/ARP132.

Conflicts of Interest: The authors declare no conflict of interest.

Abbreviations

AEMO	Australian Energy Market Operator
BESS	Battery Energy Storage System
FOS	Frequency Operating Standards
ISP	Integrated System Plan
MRL	Minimum Reserve Level
NEM	National Electricity Market
NREL	National Renewable Energy Laboratory
NSGS	Non-Synchronous Generating Sources
OFGS	Over-Frequency Generation Shedding
PFC	Primary Frequency Control
QLD	Queensland
QNI	QLD–New South Wales Interconnection
RE	Renewable Energy
ROCOF	Rate-of-Change of Frequency
SG	Synchronous Generators
UFLS	Under-Frequency Load-Shedding
VSC	Voltage Source Converter
$\dot{\Delta f}$	Rate-of-Change of Frequency (Hz/s)
f_0	Nominal frequency (Hz)
P_g	Mechanical input power (MW)
P_e	Electrical output power (MW)
P^*	Pre-set output power (MW)
S_{sys}	Base electrical power of the system (MVA)
H_{sys}	Inertia constant of the system (s)
H_m	Inertia constant of the mth unit(s)
E_{k_stored}	Stored kinetic energy of a synchronous machine rotor (MWs)
ω	Rotational speed of a synchronous machine rotor (rad/s)
J	Moment of inertia of a synchronous machine rotor (kg/m^2)
S_{rated}	Nominal power rating of a synchronous machine rotor (MVA)
S_m	Base electrical power of the mth unit (MVA)
R_{BESS}	Droop constant of BESS (pu)
R_m	Droop constant of the mth unit (pu)
Δf_{ss}	Steady-state frequency difference (Hz)

References

1. Teske, S.; Dominish, E.; Ison, N.; Maras, K. *Renewable Energy for Australia–Decarbonising Australia's Energy Sector within One Generation*; Institute for Sustainable Futures: Warriewood, Australia, 2016.
2. Institute for Sustainable Futures. Integrated System Plan. 2020. Available online: https://aemo.com.au/-/media/files/major-publications/isp/2020/final-2020-integrated-system-plan.pdf?la=en (accessed on 10 February 2021).
3. Institute for Sustainable Futures. Integrated System Plan. 2018. Available online: https://www.aemo.com.au/-/media/Files/Electricity/NEM/Planning_and_Forecasting/ISP/2018/Integrated-System-Plan-2018_final.pdf (accessed on 10 February 2021).
4. Australian Energy Market Operator. Power System Frequency Risk Review—Stage 2 Final Report. Available online: https://aemo.com.au/-/media/files/stakeholder_consultation/consultations/nem-consultations/2020/psfrr/stage-2/2020-psfrr-stage-2-final-report.pdf?la=en (accessed on 10 February 2021).
5. Oudalov, A.; Chartouni, D.; Ohler, C. Optimizing a Battery Energy Storage System for Primary Frequency Control. *IEEE Trans. Power Syst.* **2007**, *22*, 1259–1266. [CrossRef]
6. Datta, U.; Kalam, A.; Shi, J. Battery Energy Storage System Control for Mitigating PV Penetration Impact on Primary Frequency Control and State-of-Charge Recovery. *IEEE Trans. Sustain. Energy* **2020**, *11*, 746–757. [CrossRef]
7. Tuladhar, A. Power Management of an Off-Grid PV Inverter System with Generators and Battery Banks. In Proceedings of the IEEE Power and Energy Society General Meeting, Detroit, MI, USA, 24–28 July 2011; pp. 1–5.
8. Hosseinzadeh, M.; Salmasi, F.R. Power management of an isolated hybrid AC/DC micro-grid with fuzzy control of battery banks. In *IET Renewable Power Generation*; Institution of Engineering and Technology: Stevenage, UK, 2015; Volume 9, pp. 484–493.
9. Lee, S.; Kim, J.; Kim, C.; Kim, S.; Kim, E.; Kim, D.; Mehmood, K.K.; Khan, S.U. Coordinated Control Algorithm for Distributed Battery Energy Storage Systems for Mitigating Voltage and Frequency Deviations. *IEEE Trans. Smart Grid* **2016**, *7*, 1713–1722. [CrossRef]
10. Zhao, T.; Parisio, A.; Milanović, J.V. Distributed Control of Battery Energy Storage Systems for Improved Frequency Regulation. *IEEE Trans. Power Syst.* **2020**, *35*, 3729–3738. [CrossRef]
11. Amin, M.R.; Negnevitsky, M.; Franklin, E.; Naderi, S.B. Frequency Response of Synchronous Generators and Battery Energy Storage Systems: A Comparative Study. In Proceedings of the 29th Australasian Universities Power Engineering Conference (AUPEC), Nadi, Fiji, 26–29 November 2019; pp. 1–6.
12. Farrokhabadi, M.; König, S.; Cañizares, C.A.; Bhattacharya, K.; Leibfried, T. Battery Energy Storage System Models for Microgrid Stability Analysis and Dynamic Simulation. *IEEE Trans. Power Syst.* **2018**, *33*, 2301–2312. [CrossRef]
13. Gundogdu, B.M.; Nejad, S.; Gladwin, D.T.; Foster, M.P.; Stone, D.A. A Battery Energy Management Strategy for U.K. Enhanced Frequency Response and Triad Avoidance. *IEEE Trans. Ind. Electron.* **2018**, *65*, 9509–9517. [CrossRef]
14. Datta, U.; Kalam, A.; Shi, J. Battery energy storage system for transient frequency stability enhancement of a large-scale power system. In Proceedings of the Australasian Universities Power Engineering Conference (AUPEC), Melbourne, Australia, 19–22 November 2017; pp. 1–5.
15. Talaq, M.A. Frequency Stability Enhancement for a System with Integrated Renewable Energy Sources and HVDC Link. In Proceedings of the International Seminar on Application for Technology of Information and Communication (iSemantic), Semarang, Indonesia, 19–20 September 2020; pp. 391–395.
16. Byrne, R.H.; Nguyen, T.A.; Copp, D.A.; Chalamala, B.R.; Gyuk, I. Energy Management and Optimization Methods for Grid Energy Storage Systems. *IEEE Access* **2018**, *6*, 13231–13260. [CrossRef]
17. Cao, J.; Du, W.; Wang, H.; McCulloch, M. Optimal Sizing and Control Strategies for Hybrid Storage System as Limited by Grid Frequency Deviations. *IEEE Trans. Power Syst.* **2018**, *33*, 5486–5495. [CrossRef]
18. Brogan, P.V.; Best, R.J.; Morrow, D.J.; McKinley, K.; Kubik, M.L. Effect of BESS Response on Frequency and RoCoF During Underfrequency Transients. *IEEE Trans. Power Syst.* **2019**, *34*, 575–583. [CrossRef]
19. *VPP Demonstration FCAS Specification*; Australian Energy Market Operator: Melbourne, Australia, 2019.
20. Saadat, H. *Power System Analysis*; McGraw-Hill: Singapore, 1999; Volume 232.
21. Teng, F.; Trovato, V.; Strbac, G. Stochastic Scheduling With Inertia-Dependent Fast Frequency Response Requirements. *IEEE Trans. Power Syst.* **2016**, *31*, 1557–1566. [CrossRef]
22. Kundur, P.; Balu, N.J.; Lauby, M.G. *Power System Stability and Control*; McGraw-Hill: New York, NY, USA, 1994; Volume 7.
23. Riesz, J. *The Future Power System Security Program*; Australian Energy Market Operator: Melbourne, Australia, 2016.
24. Inertia Requirements Methodology Inertia Requirements and Shortfalls. Available online: https://www.aemo.com.au/-/media/Files/Electricity/NEM/Security_and_Reliability/System-Security-Market-Frameworks-Review/2018/Inertia_Requirements_Methodology_PUBLISHED.pdf (accessed on 18 August 2020).
25. Preliminary Report Non-Credible Separation Event South Australia -Victoria on 16 November 2019. Available online: https://www.aemo.com.au/-/media/Files/Electricity/NEM/Market_Notices_and_Events/Power_System_Incident_Reports/2019/Preliminary-Incident-Report---16-November-2019---SA---VIC-separation.pdf (accessed on 17 August 2020).
26. Reliability Panel. *Review of the Frequency Operating Standard*; Technical Report REL0065; Australia Energy Market Commission: Sydney, Australia, 2017.
27. Gevorgian, V.; Shah, S.D.; Martinez, A. Validation and Testing of Advanced Grid Services by Inverter-Coupled Resources. Available online: https://www.nrel.gov/docs/fy20osti/75479.pdf (accessed on 22 October 2020).

28. Final Report–Queensland and South Australia System Separation on 25 August 2018. Available online: https://www.aemo.com.au/-/media/files/electricity/nem/market_notices_and_events/power_system_incident_reports/2018/qld---sa-separation-25-august-2018-incident-report.pdf?la=en&hash=49B5296CF683E6748DD8D05E012E901C (accessed on 1 June 2020).
29. 2019 Input and Assumption Workbook. Available online: https://aemo.com.au/energy-systems/electricity/national-electricity-market-nem/nem-forecasting-and-planning/scenarios-inputs-assumptions-methodologies-and-guidelines (accessed on 18 August 2020).
30. Chown, G.; Wright, J.; van Heerden, R.; Coker, M. System inertia and Rate of Change of Frequency (RoCoF) with increasing non-synchronous renewable energy penetration. In Proceedings of the 8th CIGRE Southern Africa Regional Conference, Cape Town, South Africa, 14–17 November 2017.
31. *Rate of Change of Frequency (RoCoF) Withstand Capability*; European Network of Transmission System Operators for Electricity: Brussels, Belgium, 2017.
32. Amin, M.R.; Aizam Zulkifli, S. A framework for selection of grid-inverter synchronisation unit: Harmonics, phase-angle and frequency. *Renew. Sustain. Energy Rev.* **2017**, *78*, 210–219. [CrossRef]
33. Power System Frequency Risk Review Final Report. Available online: https://www.aemo.com.au/-/media/Files/Electricity/NEM/Planning_and_Forecasting/PSFRR/2018_Power_System_Frequency_Risk_Review-Final_Report.pdf (accessed on 18 August 2020).